Benchmarking a First-Principles Thermal Neutron Scattering Law for Water Ice with a Diffusion Experiment

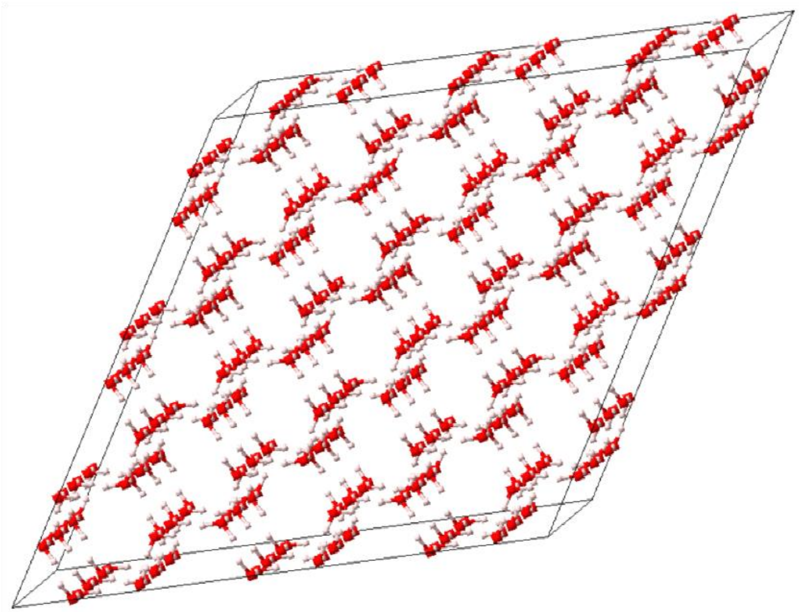

Jesse C. Holmes[1]

Michael L. Zerkle[1]

David P. Heinrichs[2]

[1] Bettis Atomic Power Laboratory
West Mifflin, Pennsylvania USA

[2] Lawrence Livermore National Laboratory
Livermore, California USA

International Conference on Nuclear Data for Science and Technology

ND2016

Bruges, Belgium

September 11-16, 2016

Motivation
(why ice?)

1. Criticality safety analyses routinely examine the reactivity effect of a liquid water environment during the transport and storage of nuclear fuel material.

2. For cold weather conditions, it is of interest to have a thermal neutron scattering law (TSL) for water ice which characterizes the impact of the chemically bound crystalline structure on neutron scattering and reflection.

3. The thermal scattering kernel for liquid water has been extensively studied and is available in an ENDF library. However, no published ENDF File 7 TSL for water ice exists.

4. Crystalline ice is a much better reflector than liquid water, although it is a poorer moderator than liquid water. Modifying the material density of liquid water to account for ice formation will not capture these effects in benchmark calculations.

The Structure of Hexagonal Ice I*h*

- H_2O molecules are bound by strong covalent bonds internally. Weak intermolecular hydrogen bonds allow for many rotational configurations of the H_2O molecules in ice on a fixed oxygen lattice.

- Ice I*h* is the most common form of H_2O ice. This structure can be viewed as two superimposed hexagonal lattices, where each lattice site contains an oxygen. The molecular alignments are locally ordered but globally disordered.

- Ice I*h* has 4 molecules per unit cell (green trapezoid). Larger unit cells can be defined to better capture the varying H_2O alignments. The red diamond is a 2-D view of the 12-molecule 3-D unit cell used in this work (top right image).

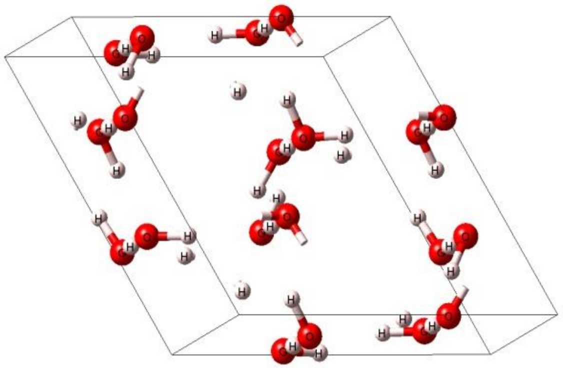

3-D view of the ice I*h* structure.

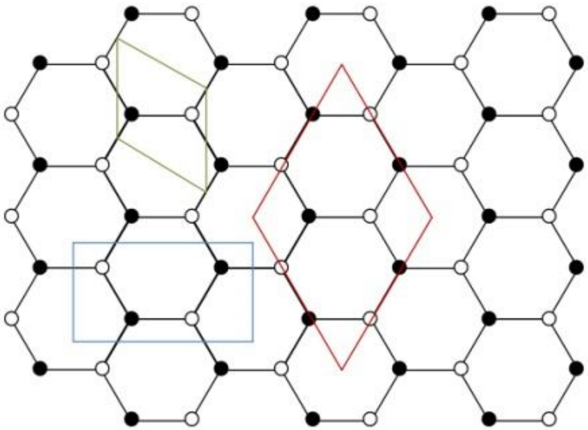

2-D view of the ice I*h* oxygen lattice.

Objectives

1. Use the VASP *ab initio* density functional theory (DFT) code and the PHONON lattice dynamics code to model the interatomic structure of ice I*h* and its dynamical behavior.

2. Calculate the vibrational phonon energy spectrum for ice I*h* and use this to calculate the $S(\alpha,\beta)$ TSL and integral inelastic scattering cross sections in the incoherent approximation.

3. Add in absorption and integral incoherent elastic scattering cross sections to determine the total cross sections as a function of temperature.

4. Based on experimentally measured inelastic neutron scattering spectra and total cross sections, optimize the phonon spectrum to account for the globally averaged ice I*h* structure.

5. Benchmark the ice I*h* thermal scattering kernel using MC21 against measured flux decay time eigenvalues from a pulsed-neutron die-away neutron diffusion experiment for cylinders of ice with various geometries over a range of temperatures.

Determining the Phonon Vibrational Energy Spectrum

- *Ab initio* method of modeling the structure and vibrational energy spectrum of ice I*h* using density functional theory (DFT) and lattice dynamics.

- High-accuracy experimental lattice constants for Ice I*h* were enforced to correctly model the hydrogen bond length.

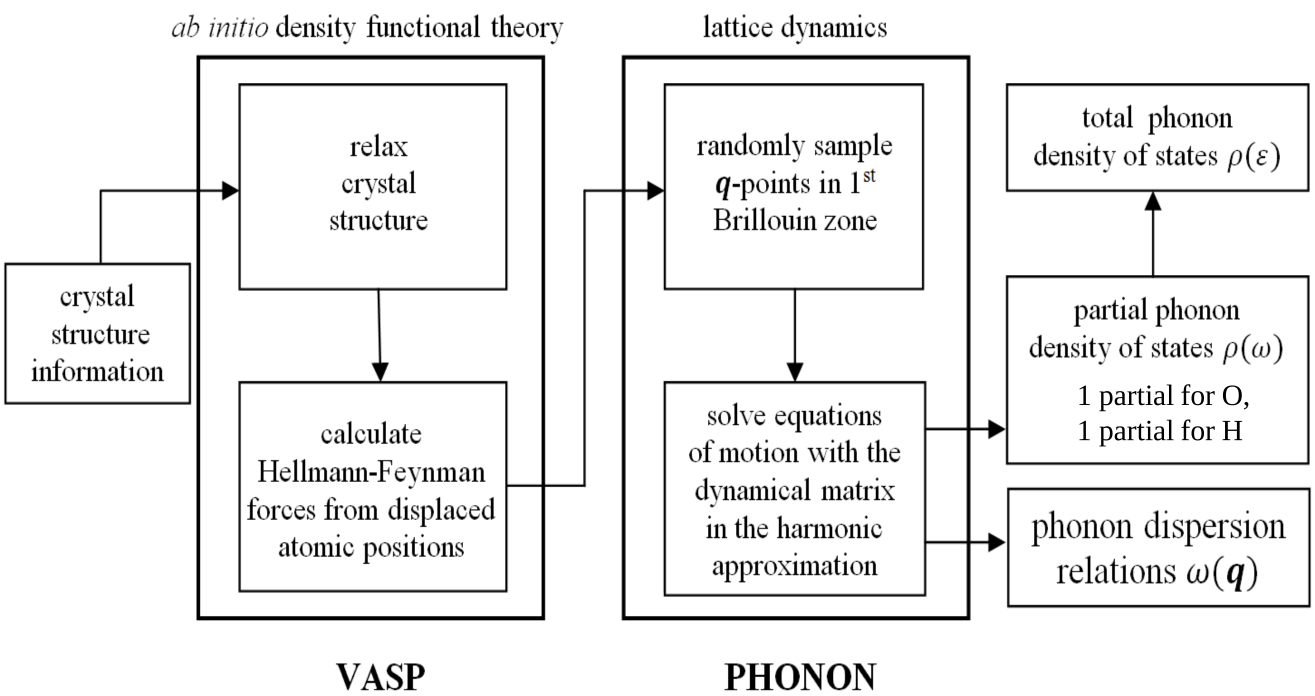

Calculated Phonon Energy Spectra

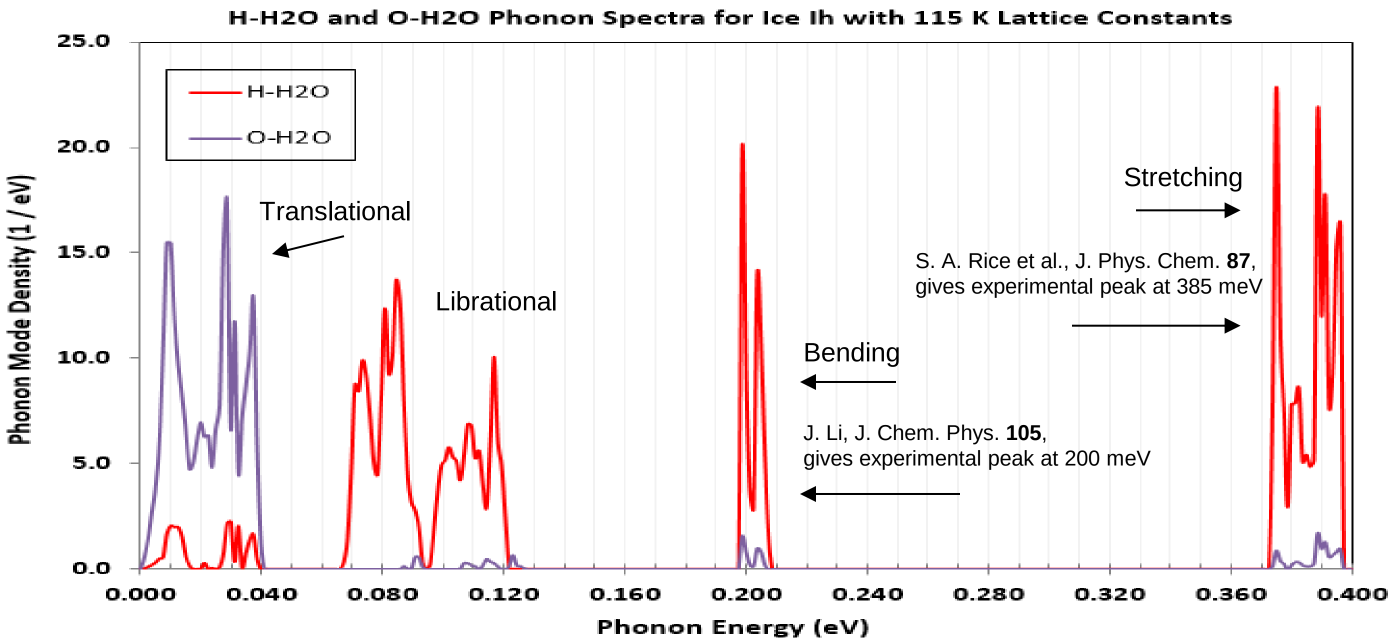

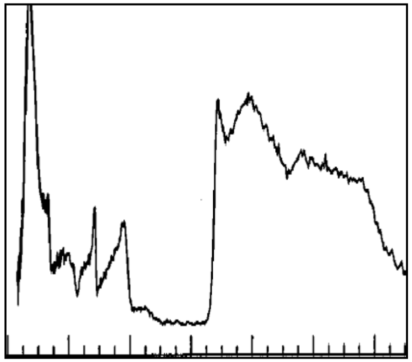

Experimental inelastic neutron scattering spectrum for polycrystalline ice I*h* (same energy scale as above).

J. Li, “Inelastic Neutron Scattering Studies of Hydrogen Bonding in Ices,” *Journal of Chemical Physics* **105**, 6733-6755 (1996).

Calculating the Thermal Neutron Scattering Kernel for Ice I*h*

$$\frac{d^2\sigma(E)}{d\alpha d\beta} = \sigma_\mathrm{b} F[S(\alpha,\beta)]$$

double-differential cross section (in angle and in energy)

The phonon energy spectrum is the fundamental parameter determining the thermal scattering law *S*(*α*,*β*) and incoherent elastic scattering for Ice I*h*.

α **momentum transfer factor (scattering angle dependence)**

β **energy transfer factor**

$$\frac{d\sigma(E)}{dE'} = \frac{1}{k_\mathrm{B}T}\frac{d\sigma(E)}{d\beta} = \int_{\alpha_{\min}(E,\beta,T)}^{\alpha_{\max}(E,\beta,T)} \frac{d^2\sigma(E)}{d\alpha d\beta} d\alpha$$

differential cross section in energy

$$\sigma(E) = \int_{\beta_{\min}(E,T)}^{\infty} \int_{\alpha_{\min}(E,\beta,T)}^{\alpha_{\max}(E,\beta,T)} \frac{d^2\sigma(E)}{d\alpha d\beta} d\alpha d\beta$$

integral inelastic cross section

$$\sigma(E) = \frac{\sigma_\mathrm{incoh}}{2}\left(\frac{1-e^{-4WE}}{2WE}\right)$$

integral incoherent elastic cross section

All cross section calculations assume the incoherent approximation. Since the nuclear bound scattering cross section for H_2O is very strongly incoherent, this is expected to yield good results for ice I*h*.

Total cross section = inelastic + elastic + absorption

Comparison of the Secondary Neutron Energy Distribution for Inelastic Scattering with Hydrogen in Water and Ice

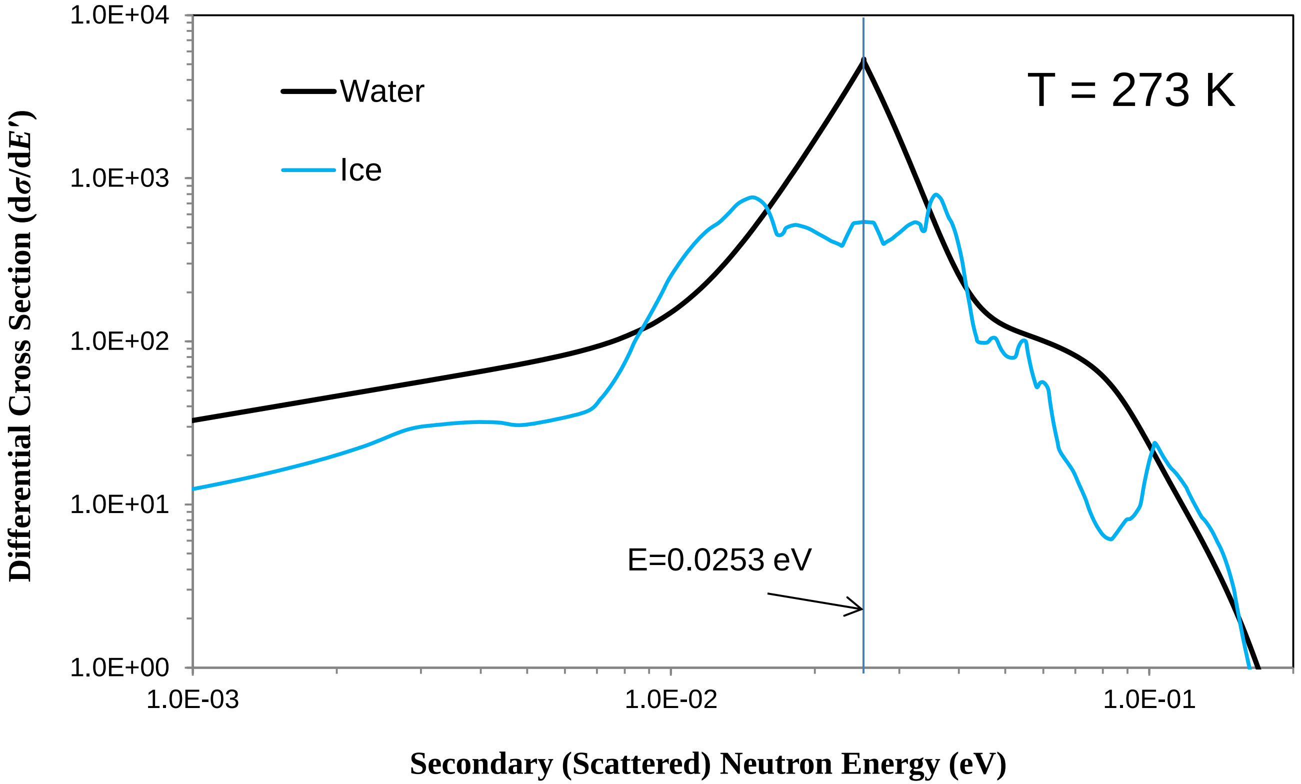

Comparison of Total and Inelastic Scattering Cross Sections for Water and Ice

Total = Inelastic + Elastic + Absorption

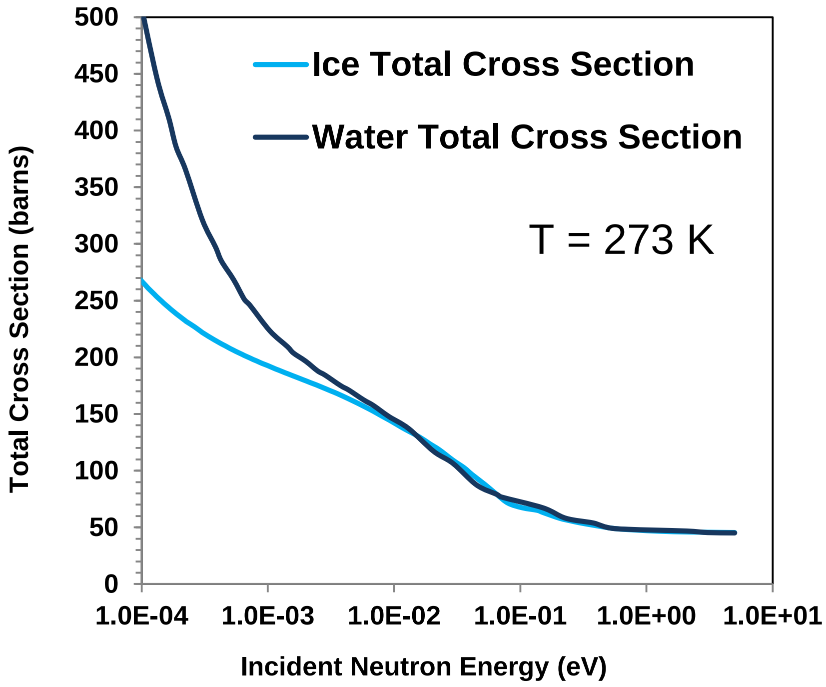

Inelastic Only
(There is no elastic scattering in liquid water)

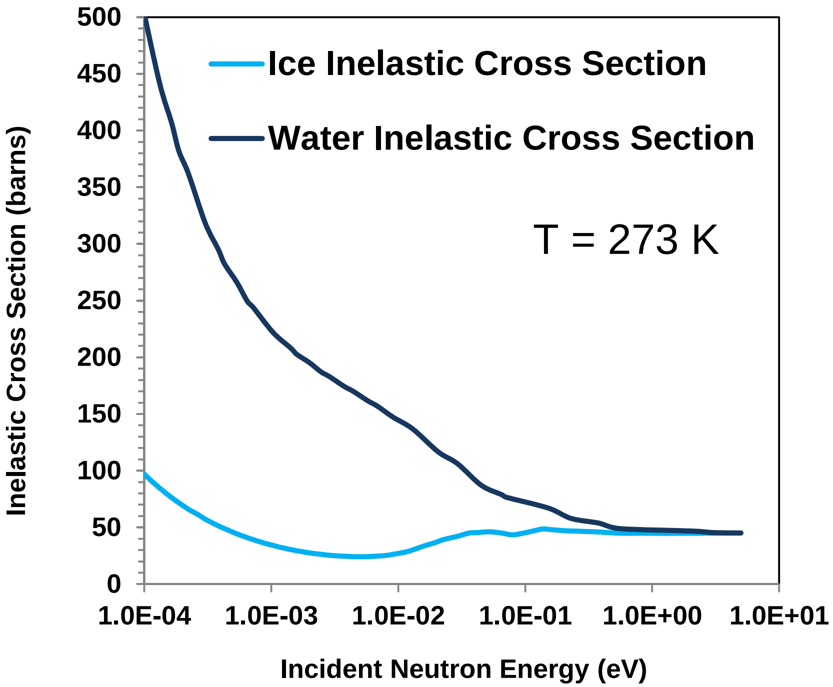

Components of Thermal Neutron Scattering Cross Sections for Ice I*h* at 115 K and 273 K

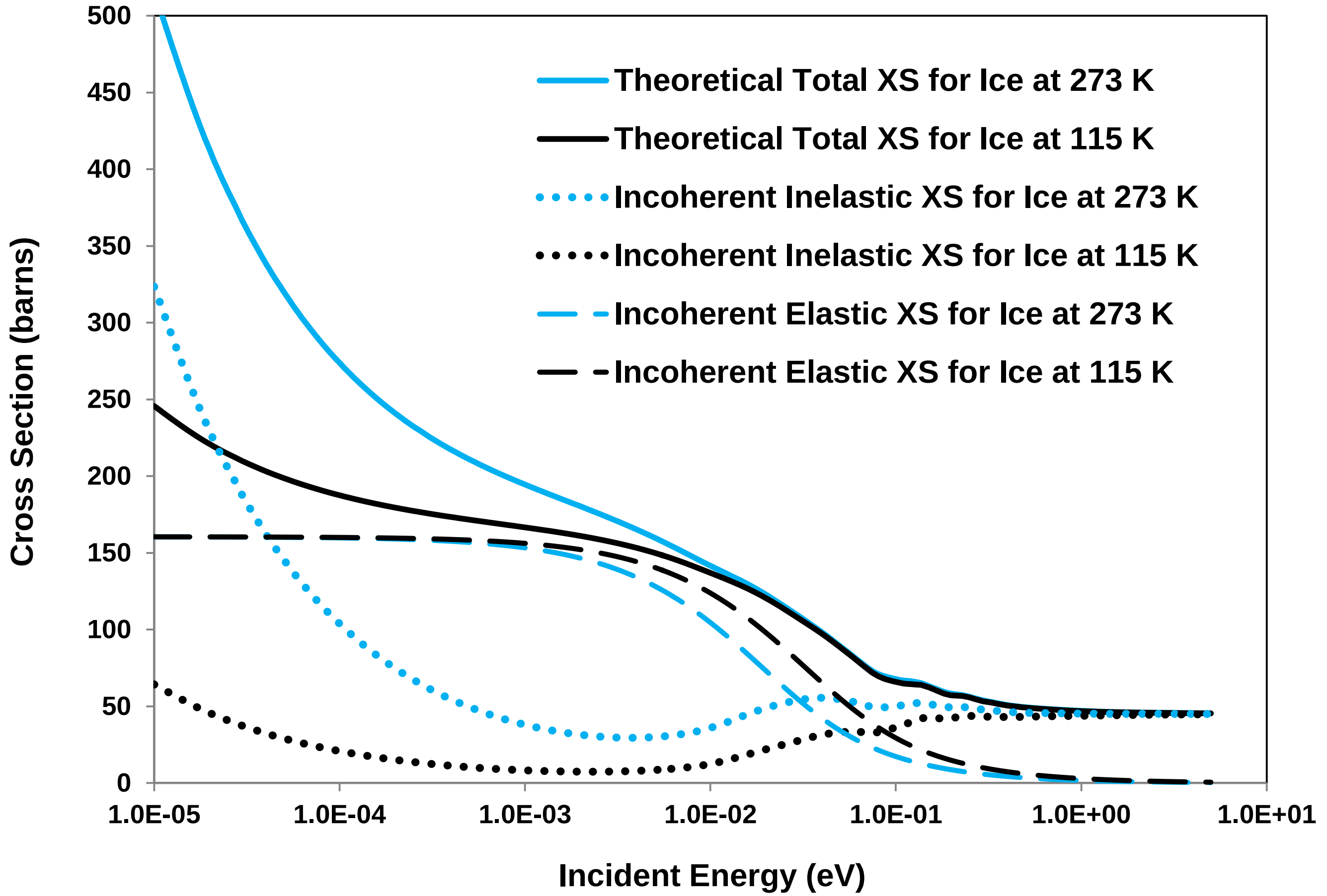

Comparison of Theoretical and Experimental Total Cross Sections for Ice I*h*

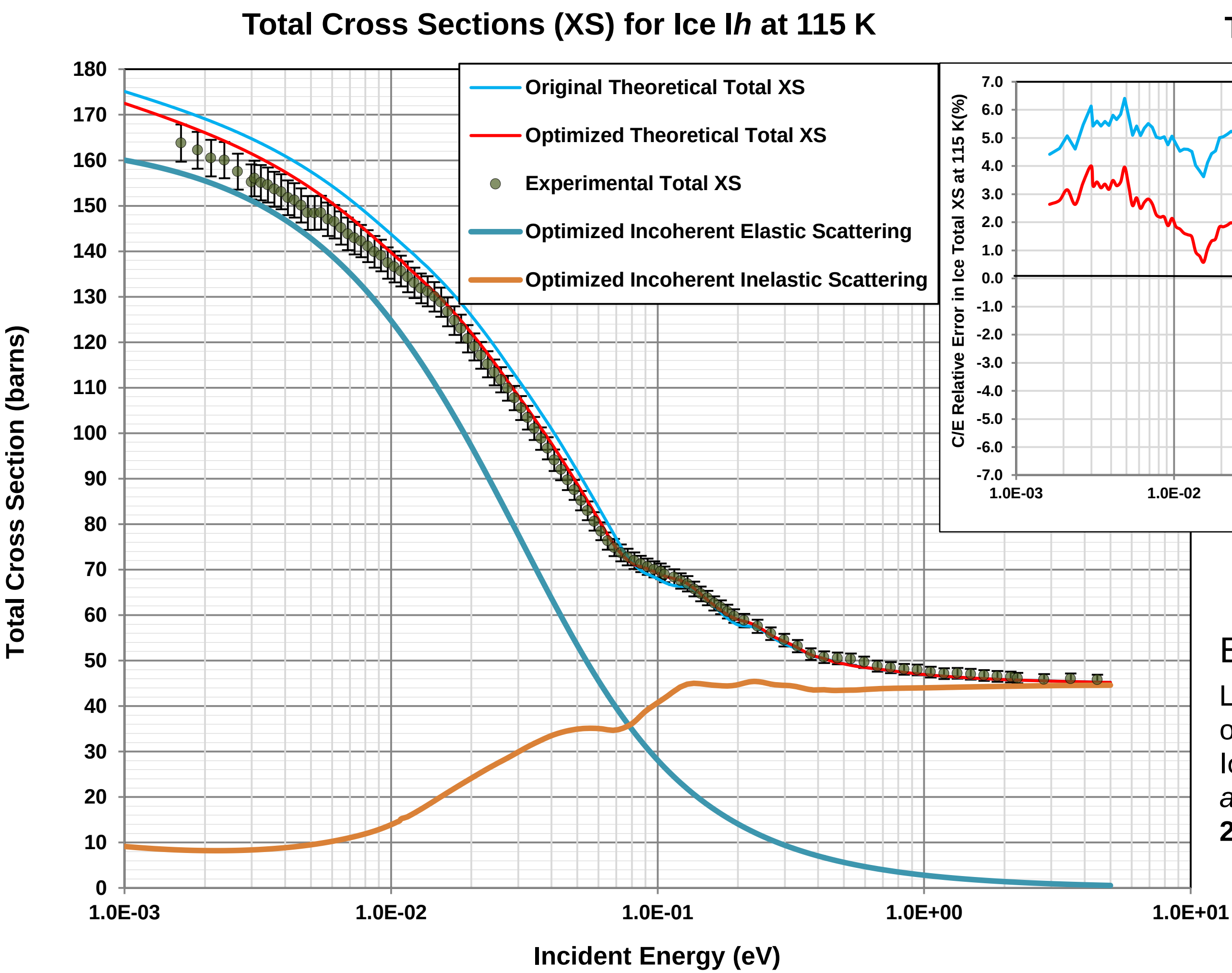

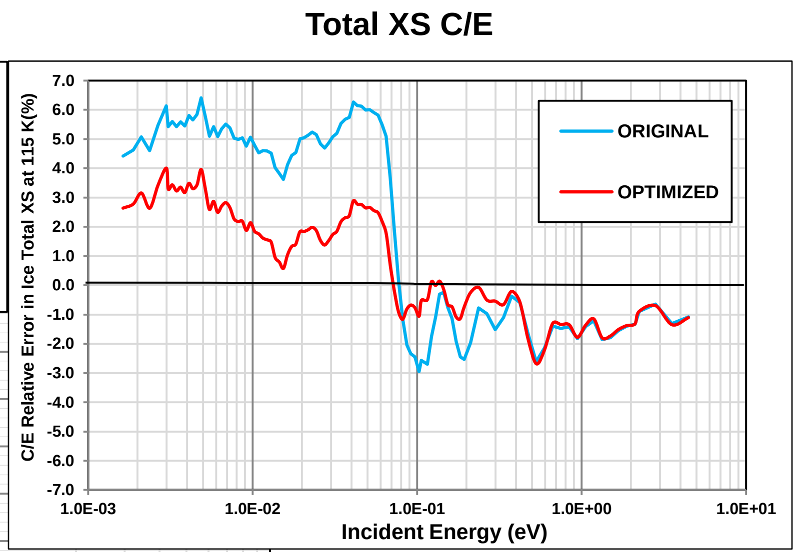

Experimental data from:

L. Torres et al., "Total Cross Sections of Benzene at 90 K and Light Water Ice at 115 K," *Nuclear Instruments and Methods in Physics Research B* **251**, 304-305 (2006).

Benchmarking the Ice I*h* Thermal Scattering Kernel with a Neutron Diffusion Experiment

- It is desirable to test the performance of the thermal neutron scattering kernel for Ice I*h* in an integral benchmark over a range of temperatures. As no critical benchmarks designed to test water ice exist, a neutron diffusion benchmark will be incorporated.

- E. G. Silver measured the diffusion parameters of Ice I*h* in the 1960s using a pulsed-neutron die-away experiment to determine the fundamental mode flux decay time eigenvalues for various-sized cylinders of ice over a range of temperatures.

- MC21 is used to test the Ice I*h* scattering kernel. NDEX reads ENDF File 7 and generates a thermal library for MC21. The ice cylinders were modeled and the resulting time eigenvalues for flux decay after an initial neutron pulse were determined and compared to experiment.

- Finally, to test the sensitivity of the benchmark to a correct scattering kernel for Ice I*h*, additional tests were performed using a subcooled liquid water library at ice density and using a free gas library at ice density.

Benchmark experimental reference:

E. G. Silver, "A Pulsed-Neutron Investigation of the Effect of Temperature on the Decay of a Thermal-Neutron Population in H_2O Ice," *Nuclear Science and Engineering* **34**, 275-284 (1968).

The Diffusion Experiment and Diffusion Theory

- A high-voltage deuteron accelerator was used with a deuterium target placed adjacent to the ice cylinder. A pulse of high-energy neutrons was produced and an adjacent lithium iodide detector and time channel analyzer were used to record the flux decay. Data was collected over many pulses.

- After sufficient waiting time following the initial pulse, the neutron population is in thermal equilibrium and settles into the fundamental spatial mode with a single flux decay time eigenvalue.

- In the one-speed diffusion model, the flux decay of the fundamental spatial mode can be expressed as

$\varphi(\mathbf{r},t) = \varphi_0(\mathbf{r}) \exp[-(v\Sigma_a + vDB^2 - CB^4)t]$, where the time eigenvalue $\alpha = v\Sigma_a + vDB^2 - CB^4$

Σ_a is the macroscopic absorption cross section
$D = 1/\Sigma_{transport}$ is the diffusion parameter,
v = the effective average neutron velocity,
B^2 = geometric buckling, and
C = the diffusion cooling parameter

While the analytical form for the α time eigenvalue is approximate, we should expect that small geometries with high buckling should be very sensitive to the TSL supplied and large geometries with low buckling should be relatively insensitive to the TSL.

Benchmark Testing Results

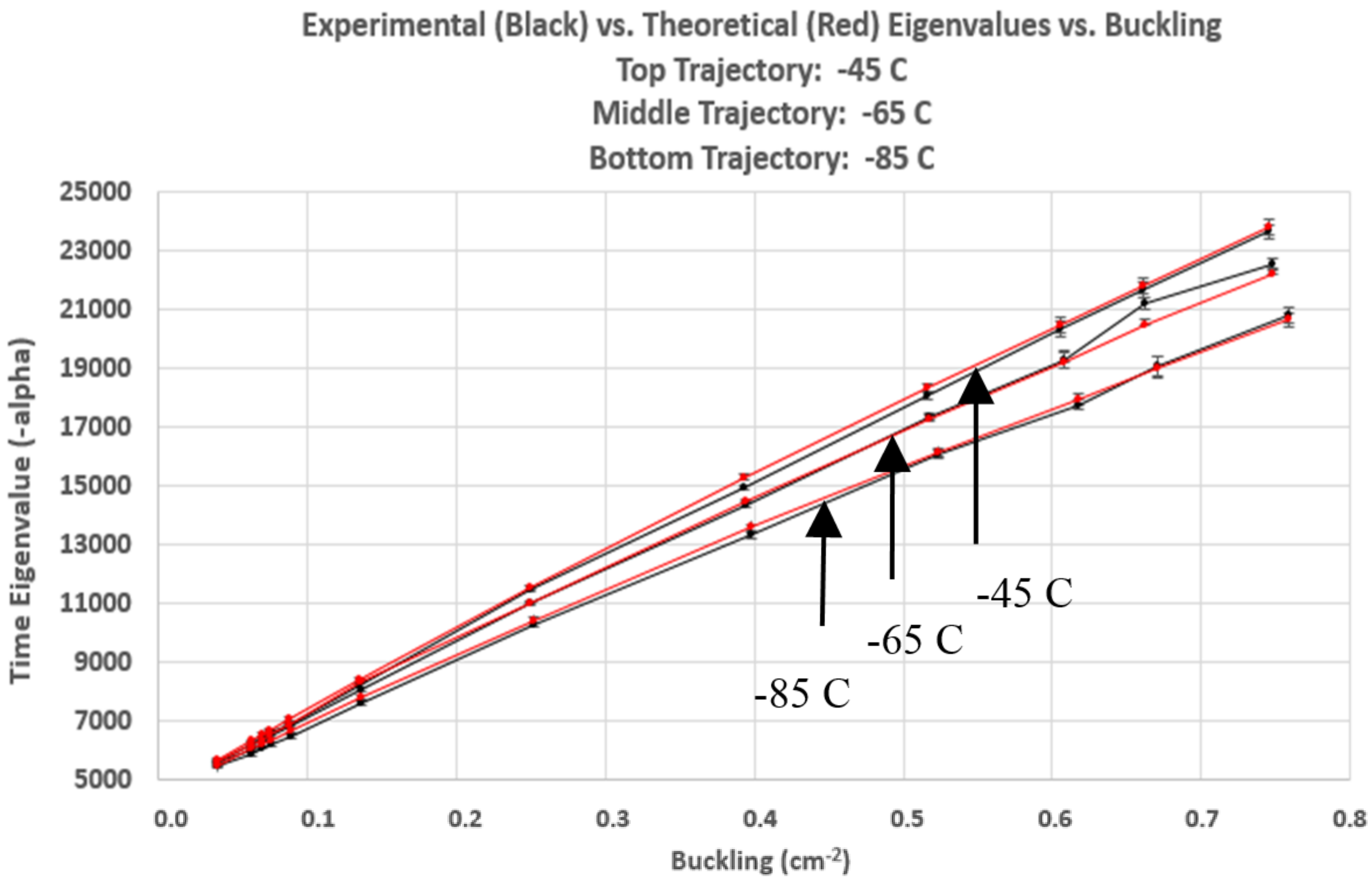

Benchmark Testing Results

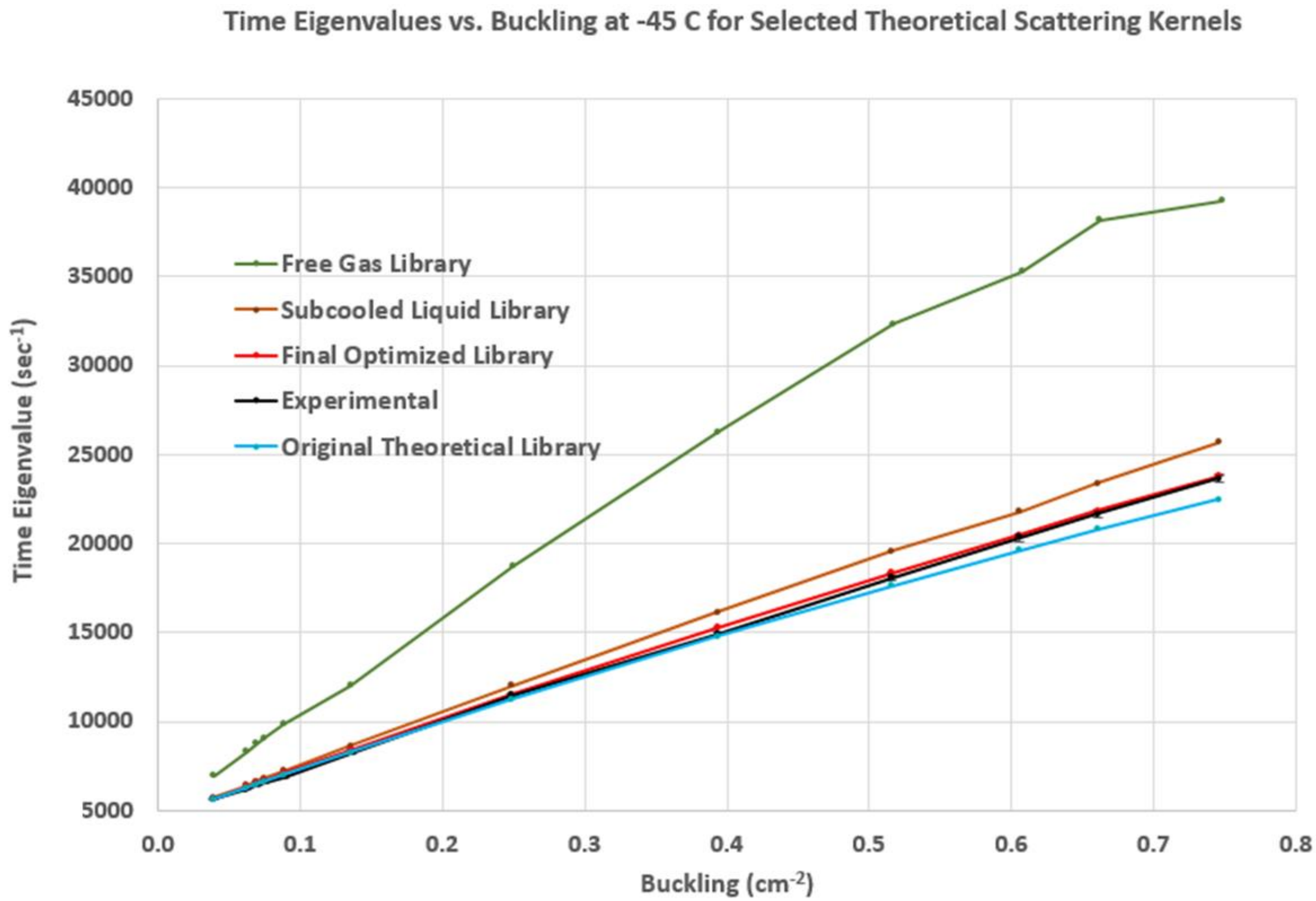

Benchmark Testing Results

SILVER EXPERIMENTAL									FINAL LIBRARY (-45 C)				FINAL LIBRARY (-65 C)				FINAL LIBRARY (-85 C)			
-45 C			-65 C			-85 C			MC21 α	σ	C/E	σ	MC21 α	σ	C/E	σ	MC21 α	σ	C/E	σ
B^2	α	σ	B^2	α	σ	B^2	α	σ												
0.0394	5630	52	0.0395	5579	59	0.0396	5443	35	5659	6	1.0051	0.009	5589	3	1.0018	0.009	5504	3	1.0112	0.007
0.0621	6207	38	0.0621	6031	35	0.0624	5890	61	6325	5	1.0191	0.006	6190	4	1.0264	0.006	6057	1	1.0284	0.011
0.0689	6413	66	0.0690	6266	22	0.0693	6096	53	6523	2	1.0172	0.010	6370	2	1.0166	0.010	6217	4	1.0199	0.009
0.0748	6584	70	0.0749	6455	38	0.0752	6226	66	6697	2	1.0171	0.011	6530	2	1.0117	0.011	6365	2	1.0223	0.011
0.0880	6888	49	0.0881	6825	76	0.0885	6493	72	7074	3	1.0270	0.007	6876	3	1.0075	0.007	6682	2	1.0290	0.011
0.1352	8214	70	0.1354	8052	73	0.1362	7593	72	8415	3	1.0244	0.009	8356	5	1.0377	0.009	7804	3	1.0278	0.010
									Low B^2 Avg. C/E		1.0183		Low B^2 Avg. C/E		1.0169		Low B^2 Avg. C/E		1.0231	
0.2490	11493	87	0.2494	10997	76	0.2514	10272	82	11546	12	1.0046	0.008	10985	10	0.9989	0.008	10427	8	1.0150	0.008
0.3933	14915	73	0.3941	14341	65	0.3981	13310	100	15302	56	1.0259	0.006	14458	43	1.0082	0.006	13598	33	1.0216	0.008
0.5161	18083	127	0.5174	17307	132	0.5233	16055	129	18350	59	1.0148	0.008	17259	45	0.9972	0.008	16158	47	1.0064	0.009
0.6058	20349	245	0.6078	19292	295	0.6172	17772	189	20482	52	1.0065	0.012	19232	39	0.9969	0.012	17952	30	1.0102	0.011
0.6606	21669	258	0.6624	21226	195	0.6710	19073	344	21818	104	1.0069	0.013	20449	77	0.9634	0.013	19033	57	0.9979	0.018
0.7460	23662	229	0.7482	22555	198	0.7586	20808	236	23795	105	1.0056	0.011	22199	77	0.9842	0.011	20663	57	0.9930	0.012
									High B^2 Avg. C/E		1.0107		High B^2 Avg. C/E		0.9915		High B^2 Avg. C/E		1.0074	

For the six highest buckling geometries (B^2 is in units of cm^{-2}), which are the most sensitive to the supplied thermal scattering kernel, the average C/E across all three temperatures is 1.003.

For the six lowest buckling geometries, the average C/E across all three temperatures is 1.019. As these cases are relatively insensitive to the supplied thermal scattering kernel, this indicates there may be a slight positive bias in the absorption cross sections. Indeed, this is consistent with the ~2.5% ENDF quoted uncertainty for H absorption cross sections in the thermal energy range.

Summary / Conclusions

- While the total cross sections for liquid water and solid ice are similar (except at extremely low incident energies), the details of the scattering kernels differ significantly and result in significant differences in the diffusion of neutrons through the material.

- Unlike liquid water, a large fraction of neutron scattering that takes place in ice is elastic. Consequently, Ice I*h has* enhanced reflective properties over liquid water that could have important criticality safety implications.

- Combining the first-principles VASP/PHONON methodology with experimentally measured scattering data and a diffusion benchmark has resulted in the development and successful testing of a thermal neutron scattering kernel for Ice I*h.*

- A full ENDF File 7 thermal neutron scattering library will be submitted to the National Nuclear Data Center for the ice I*h* structure for a range of temperatures of interest.